

High Order Diffraction Suppression of the Membrane with Hexagonal Hole Array

Ziwei Liu^{1,2,3}, Lina Shi^{1,2}, Tanchao Pu^{1,2,3}, Changqing Xie^{1,2}, Hailiang Li^{1,2} and Jiebin Niu^{1,2}

¹Key Laboratory of Microelectronic Devices & Integrated Technology,

Institute of Microelectronics of Chinese Academy of Sciences, Beijing 100029, China

²Jiangsu National Synergetic Innovation Center for Advanced Materials, Nanjing 210009, China

³University of Chinese Academy of Sciences, Beijing 101408, China

Keywords: Diffraction Gratings, Binary Optics, Optical Design Fabrication, Spectroscopy, High-Resolution.

Abstract: We propose the array of hexagonal holes with the completely suppression of the 2nd, 3rd, and 4th order diffractions. The membrane with holes can be free-standing and scalable from X-rays to far infrared wavelengths. We numerically and experimentally demonstrate that the 2nd, 3rd and 4th order diffractions near the 1st order diffraction are completely suppressed. The hexagonal hole with some size results in a desired diffraction pattern. Our results should be of great interest in a wide spectrum unscrambling for any wavelength range.

1 INTRODUCTION

Diffraction gratings are optical components with a periodic structure, which disperse different wavelengths of light into its constituent spectrum. They play a crucial role in modern optical science, especially in extreme-ultraviolet and soft x-ray regions. Over a period of several decades, the applications of diffraction gratings are extensively used in astrophysical plasma diagnosis and synchrotron radiation light monochromator (K. P. Beuermann, 1998; Y. Saitoh, 2000). Normally, conventional diffraction gratings are used as dispersion elements in spectral measurement, the diffracted beams corresponding to consecutive orders may overlap, depending on the spectral content of the incident beam and the grating density (V. Daneu, 2000; I. Shoshan, 1977). The higher the spectral order, the greater the overlap into the next order (V. Daneu, 2000; I. Shoshan, 1977; K. Yamane, 2003; Y. W. Huang, 2004). However, in many applications, only the first order is meaningful and necessary. The data obtained with this grating due to the high-order diffraction contamination will decrease the accuracy of spectral data. The single-order diffractions with accurate spectroscopic data have been the major concern.

Sinusoidal amplitude transmission gratings (STGs) can suppress the high-order diffraction efficiently which have only 0th- and $\pm 1^{st}$ order diffractions in a visible light region, but it's hard

to extend to x-ray region. Due to the all known materials in the extreme ultraviolet and x-ray regions have complex refractive index and are very close to unity. The fabrication with high line density grating is difficult to achieve according today's nanofabrication technology. In recent years, many new gratings which have quasi-sinusoidal transmission functions have been designed to solve this problem, but still limited to the modern photolithography technology, especially for applications in the extreme-ultraviolet and x-ray regions. The pattern structure of the gratings is recognized by many as the key to suppress high-order diffraction effectively and decrease the difficulty of fabrication.

In this Letter, we introduce a novel design of single-order diffraction which can suppress high-order diffraction significantly as sinusoidal amplitude gratings do. The key idea is to make the hexagonal holes follow the rectangle array, leading to dominant $\pm 1^{st}$ diffraction orders on the observation line (M. Born, 1997; L. Cao, 2007; L. Kuang, 2010; M. E. Warren, 1995; G. Vincent, 2008). Compared with the previous schemes, the single-order diffraction grating with binary transmittance value of 0 and 1 based on this kind of transmission function (F. J. Torcal-Milla, 2008; C. Xie, 2010; C. Xie, 2012), which is larger than the value of 6.25% for ideal sinusoidal amplitude grating. This new type of single optical element with the capabilities of quasi-single order diffraction named hexagonal aperture gratings

(HAGs) as shown in Figure 1, consists of a series of periodically arranged hexagonal apertures. Such structure has great advantages in extreme-ultraviolet and x-ray regions. In addition, HAGs on the glass substrate are easy to fabricate. Both numerical solution and experimental results demonstrate the diffraction efficiency of the HAGs. It offers a new idea of single-order diffraction and benefit in fabrication.

2 DESIGN AND SIMULATIONS

We start the design from the array of hexagonal holes as shown in Figure 1. The (x, y) and (η, ξ) are the coordinate systems in the hole plane and diffraction plane respectively. For a membrane that contains a large number of identical and similarly oriented holes, the light distribution in the Fraunhofer diffraction pattern is given by (W. Goodman, 1996),

$$U(p, q) = C \sum_N e^{-ik(px_n + qy_n)} \iint_A e^{-ik(px' + qy')} dx' dy' \quad (1)$$

Here $C = \sqrt{P}/(\lambda R)$, P is the power density incident on the hole array, λ is the incident light wavelength, R is the distance between the hole array plane and the diffraction plane. The coordinates of the hole center are $(x_1, y_1), (x_2, y_2), \dots, (x_N, y_N)$, and k is the wave vector. The integration extends over the hole area and the integral expresses the effect of a single hole. The sum represents the superposition of the coherent diffraction patterns.

For the square array of $N_x N_y$ hexagonal holes of the side $2a_1$ along the x axis, the diagonal $2a$ along the y axis, and the height along axis as shown in Fig. 1(a), the diffraction intensity pattern is

$$\begin{aligned} I(p, q) &= U(p, q) * U^*(p, q) \\ &= I_0 \cdot \frac{\sin^2(N_x k p P_x / 2)}{N_x^2 \cdot \sin^2(k p P_x / 2)} \cdot \frac{\sin^2(N_y k q P_y / 2)}{N_y^2 \cdot \sin^2(k q P_y / 2)} \\ &\quad \cdot \left| \frac{\cos(k p a_1 - k q b) - \cos k p a}{k p (a + a_1) \cdot (k p (a - a_1) + k q b)} \right. \\ &\quad \left. + \frac{\cos k p a - \cos(k p a_1 + k q b)}{k p (a + a_1) \cdot (-k p (a - a_1) + k q b)} \right|^2 \end{aligned} \quad (2)$$

Here $I_0 = C^2 \cdot (N_x N_y \cdot 2(a + a_1)b)^2$ is the peak irradiance of the diffraction pattern. For simplicity, here we set $I_0 = 1$, P_x and P_y (shown in Fig. 1) are respectively the periods along the x and y axes.

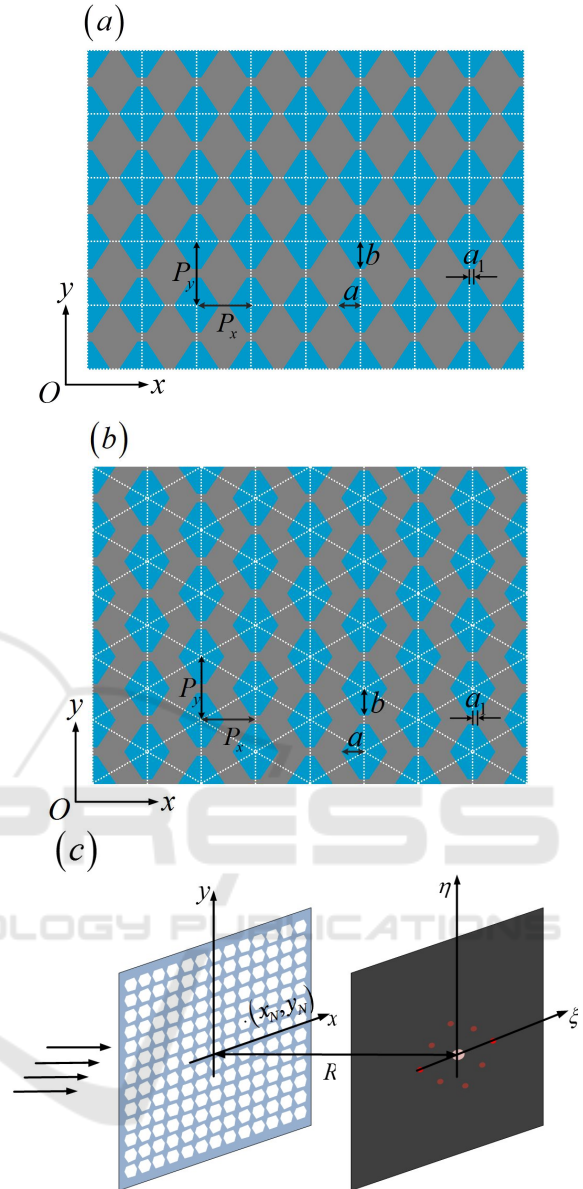


Figure 1: The array of hexagonal holes. The side along the x axis is $2a_1$, the diagonal along the x axis is $2a$ and the height along the y axis is $2b$. (a) The square array with periods P_x and P_y . (b) The triangle array with periods $2P_x$ and P_y . (c) The coordinate systems in the aperture plane and observation planes.

Similarly, for the triangle array as shown in Fig. 1(b), the diffraction intensity pattern is

$$\begin{aligned}
 I(p, q) &= U(p, q) * U^*(p, q) \\
 &= I_0 \cdot \frac{\sin^2(N_x/2 \cdot kp2P_x/2)}{(N_x/2)^2 \cdot \sin^2(kp2P_x/2)} \\
 &\quad \cdot \frac{\sin^2(N_y kqP_y/2)}{N_y^2 \cdot \sin^2(kqP_y/2)} \\
 &\quad \cdot \cos^2(kp2P_x/4 + kqP_y/4) \\
 &\quad \cdot \left| \frac{\cos(kpa_1 - kpb) - \cos kpa}{kp(a + a_1) \cdot (kp(a - a_1) + kqb)} \right. \\
 &\quad \left. + \frac{\cos kpa - \cos(kpa_1 + kqb)}{kp(a + a_1) \cdot (-kp(a - a_1) + kqb)} \right|^2 \quad (3)
 \end{aligned}$$

The parameters are same as the square array except the period $2P_x$ along the x axis.

Here, we focus on the diffraction intensity along the x axis since spectral measurement is usually at one direction. For the square and triangle arrays, the diffraction intensity according to Eq.(2) and (3) along the x axis are both given by

$$\begin{aligned}
 I(p) &= I_0 \cdot \frac{\sin^2(N_x kpP_x/2)}{N_x^2 \cdot \sin^2(kpP_x/2)} \\
 &\quad \cdot \left(\frac{\sin(kp(a + a_1)/2) \cdot \sin(kp(a - a_1)/2)}{kp(a + a_1)/2 \cdot kp(a - a_1)/2} \right)^2 \quad (4)
 \end{aligned}$$

And thus the m -th order diffraction along the x axis is

$$I(m) = I_0 \cdot \left(\frac{\sin(m(a + a_1)\pi/P_x) \cdot \sin(m(a - a_1)\pi/P_x)}{m(a + a_1)/2m(a - a_1)\pi/P_x} \right)^2 \quad (5)$$

In real spectral measurement, only the near diffractions (such as the 2^{nd} , 3^{rd} and 4^{th} order diffractions) will overlap the 1st order diffraction. The far diffractions are usually very small and have little effects on the 1^{st} order diffraction. Thus we will consider the structure parameters which lead to the zeros of the 2^{nd} , 3^{rd} and 4^{th} order diffractions. Equation (4) shows that the diffractions along the x axis have nothing to do with the parameters of b and P_y . The diffractions along the x axis depend on the parameters of a , a_1 and P_x as shown in Fig.2.

According to Equation (5) and Fig.2, the 2^{nd} , 3^{rd} and 4^{th} order diffractions $I(2) = I(3) = I(4) = 0$ as $a_1 = P_x/12$ and $a = 5P_x/12$. At the same time, the 5^{th} order diffraction $I(5) = 0.0004435I_0 = 0.0016I(1)$, the 0^{th} order diffraction $I(0) = I_0$, the 1^{st} order diffraction $I(1) = 0.2772I_0$.

Figure 3 presents the diffraction intensity pattern the array of hexagonal holes with $a_1 = P_x/12$,

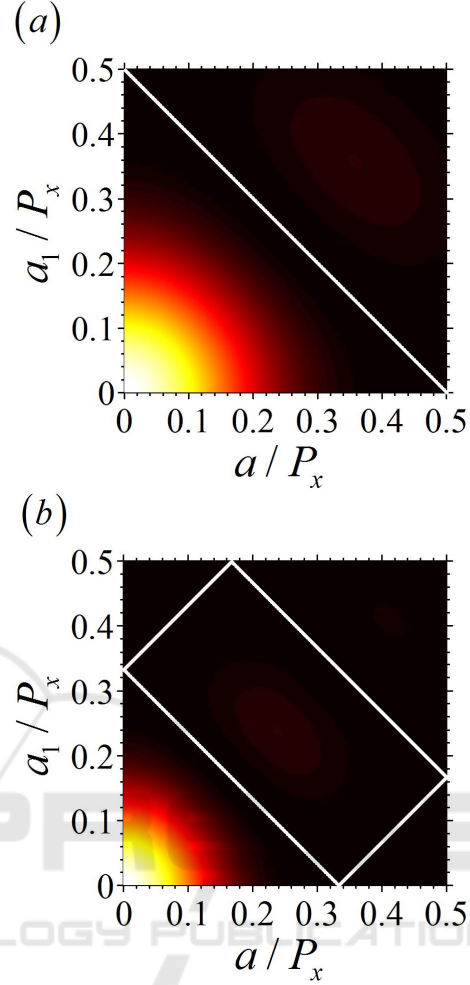


Figure 2: (a) The dependent relation of the 2^{nd} order diffraction on a, a_1 and P_x . The white line denotes the 2^{nd} order diffraction is zero. (b) The dependent relation of the 3^{rd} order diffraction on a, a_1 and P_x . The white line denotes the 3^{rd} order diffraction is zero.

$a = 5P_x/12$ and $b = P_x/12$ according to Eq.(2) and (3). Comparing with the diffraction pattern of conventional 1:1 traditional gratings(TGs), higher-order diffraction components of HAGs are suppressed by about three orders, which is weak enough for application and very similar to the ideal sinusoidal transmission gratings. As expected, the 0^{th} and 1^{st} order diffractions are kept along x axis, and the 2^{nd} , 3^{rd} and 4^{th} diffractions disappear. The logarithm of diffraction intensity along x axis in Fig.3(c) and (d) presents clearly the complete suppression of the 2^{nd} , 3^{rd} and 4^{th} order diffractions. The 5^{th} order diffraction is smaller than the noise between the 0^{th} and 1^{st} order diffractions. Insets in Fig. 3 shows clearly intensity distributions of the 0^{th} and 1^{st} order diffractions. Figure 3 shows that the high order diffractions along axis

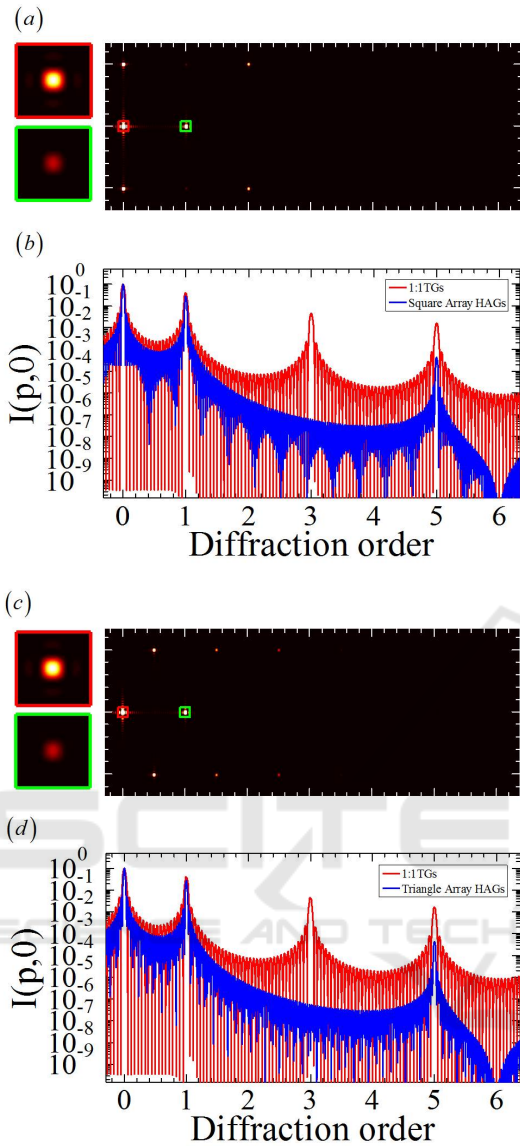


Figure 3: The far-field diffraction intensity pattern of the hexagonal hole array. The diffraction intensity along the x axis. Insets: the 0th and 1st order diffractions. (a)(b) For the square array. (c)(d) For the triangle array. (e)(f) The typical diffraction patterns by 1:1 TGs.

are effectively suppressed by the array of hexagonal holes.

Figure 3 also presents important figures of merit of the HAGs, the relative diffraction efficiency of the $\pm 1^{\text{st}}$ orders (the $+1^{\text{st}}$ or -1^{st} order diffracted light intensity divided by the 0th order diffracted light intensity) is 27.16%. For the triangle array, the relative diffraction efficiency of the $\pm 1^{\text{st}}$ orders are 27.13%. For the HAGs, the smallest feature size in both of the arrays is $4\mu\text{m}$, making it much easier to fabricate, compared with sinusoidal amplitude transmis-

sion gratings designed previously. In addition, the gap between the apertures is flexible for the practical applications, which have not effect on the result.

3 EXPERIMENTAL RESULTS AND DISCUSSION

A proof-of-principle experiment is performed to confirm our theoretical and numerical results. The square array of hexagonal holes with $4\text{cm} \times 4\text{cm}$ area is fabricated on a glass substrate by DESIGN WRITE LAZER 2000 from Heidelberg Instruments Mikrotechnik GmbH. The microphotograph of fabricated structure is illustrated in Fig.4(a) and (b). Periods P_x and P_y of the quasi-rectangle array along the x and y axes are respectively $24\mu\text{m}$ and $28\mu\text{m}$. The structure consists of 1500×1500 holes. The entirety experimental setup for optical demonstration is shown in Fig.4(c). A collimated laser beam from Sprout (Lighthouse Photonics) with wavelength of 632nm was used to illuminate the fabricated the hexagonal hole array, and the far-field diffraction pattern from the gratings was focused by a lens and then recorded on a charge coupled device (CCD) camera (ANDOR DU920P-BU2) with 1612×1214 pixels and $4.4\mu\text{m}$ pixel size was placed in the far field to record the diffraction patterns.

The measurement results are shown in Fig.5. As expected, the higher-order contributions of the fabricated HAGs are significantly suppressed. The integrated diffraction intensity of the diffraction orders along the ξ axis is shown in Fig.5(b). The relative diffraction efficiency is an important parameter for describing the characteristics of the HAGs. For perfect HAGs, it agrees well with the theoretical value, the higher-order diffraction components are significantly suppressed, which is only about 0.6% of the $\pm 1^{\text{st}}$ order in amplitude. It is obvious that only 0th and $\pm 1^{\text{st}}$ orders exist along the ξ axis, which is agrees well with the numerical simulation and the optimal case to suppress higher order diffraction is achieved. The relative diffraction efficiencies of the square array of the 1st order is 30.27%. For the triangle array, the $+1^{\text{st}}$ order is 25.82%, respectively. The experimental result differs slightly from the ideal intensity distribution shown in Fig.3. This may be attributed to the limited dynamic range and signal-to-noise ratio of the CCD, filter inhomogeneity, slightly tilted installation of the measured HAGs and the inevitable imperfection of the fabrication. Nevertheless, the experimental results clearly verify that the HAGs with quasi suppression of higher-order diffractions are superior to a conventional transmission grating.

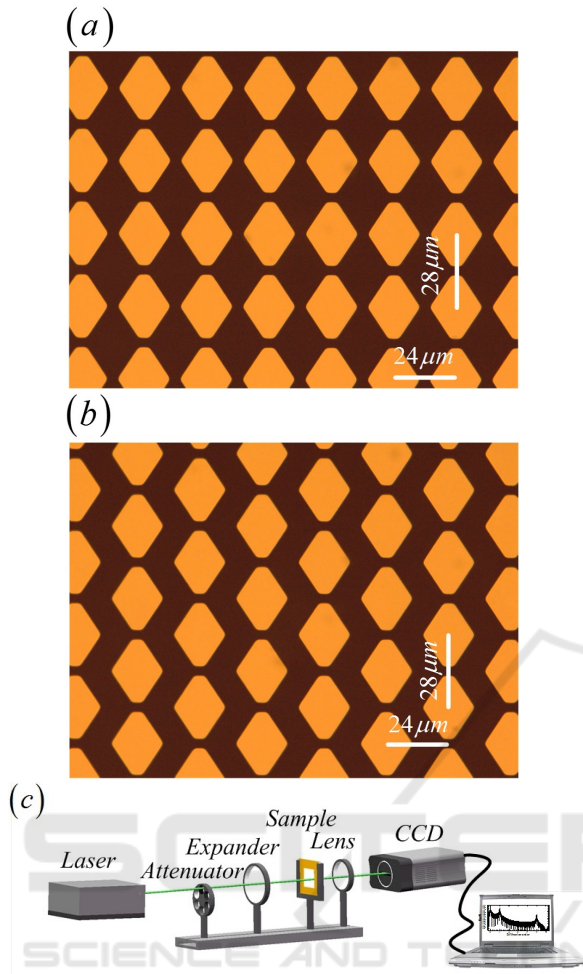


Figure 4: (a) The schematic illustration of HAGs. (b) Microphotograph of the fabricated quasi-rectangle array with $4\text{cm} \times 4\text{cm}$ area. (c) Experimental setup for the optical measurement.

4 CONCLUSIONS

In conclusion, the binary structure with hexagonal hole array has been proposed to suppress the high-order diffractions which may lead to wavelength overlapping in spectral measurement. We obtain the relative diffraction efficiency 27.72% of the first order diffraction, which is higher than 25% of the first order diffraction for ideal sine grating. The membrane with holes can be free-standing and scalable from X-rays to far infrared wavelengths. Both numerical and experimental results have demonstrated the 2nd, 3rd and 4th order diffractions are completely suppressed. The binary hole array offers an opportunity for high-accuracy spectral measurement and will possess broad potential applications in optical science and engineering fields.

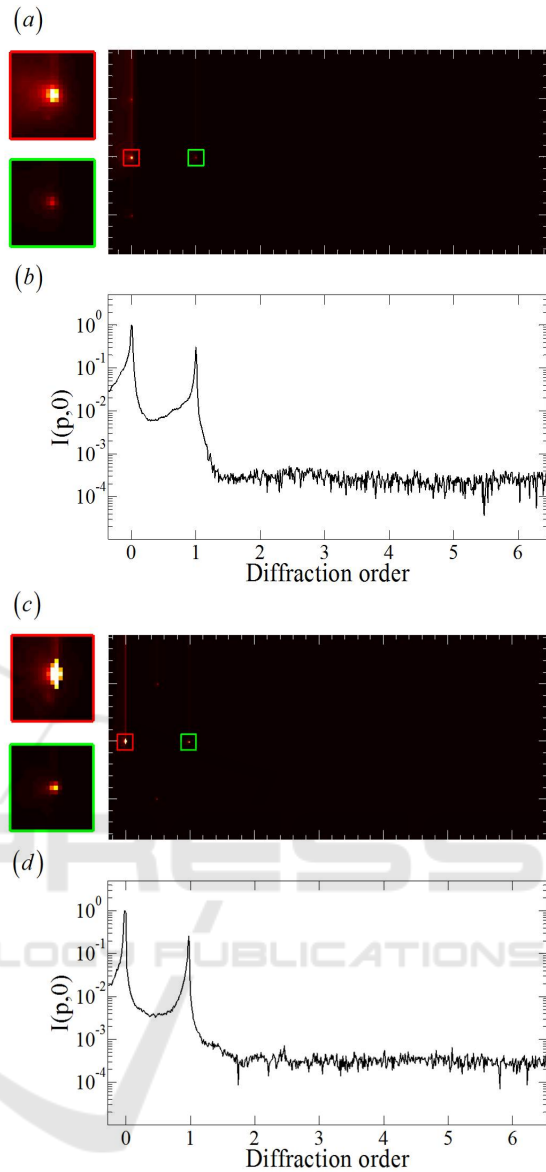


Figure 5: (a) (c) The far-field diffraction intensity pattern of the quasi-triangle array of rectangular holes. (b) (d) The diffraction intensity along the x axis.

ACKNOWLEDGEMENTS

We thank Yongliang Zhang for the valuable discussion. We thank the Optics Laboratory for the use of their equipment.

REFERENCES

C. Xie, X. Zhu, H. (2012). *Toward two-dimensional nanometer resolution hard X-ray differential-*

- interference-contrast imaging using modified photon sieves*. Opt. Lett. 37, 749-751.
- C. Xie, X. Zhu, L. S. (2010). *Spiral photon sieves apodized by digital prolate spheroidal window for the generation of hard-x-ray vortex*. Opt. Lett. 35, 1765-1767.
- F.J. Torcal-Milla, L. M. Sanchez-Brea, E. B. (2008). *Diffraction of gratings with rough edges*. Opt. Express 16, 19757.
- G.Vincent, R. Haidar, S. C. (2008). *Realization of sinusoidal transmittance with subwavelength metallic structures*. J. Opt. Soc. Am. B 25, 834.
- I. Shoshan, N. N. Danon, U. P. O. (1977). *Performance of a very high resolution soft x-ray beamline BL25SU with a twin-helical undulator at SPring-8*. Rev. Sci.Instrum. 71, 3254.
- K. P. Beuermann, R. Lenzen, H. B. (1998). *Properties of a transmission grating behind a grazing incidence telescope for cosmic x-ray spectroscopy*. Appl. Opt.16, 1425.
- K. Yamane, Z. Zhang, K. O. (2003). *Optical pulse compression to 3.4fs in the monocycle region by feedback phase compensation*. Opt. Lett. 28, 2258.
- L. Cao, E. Frster, A. F. (2007). *Single order x-ray diffraction with binary sinusoidal transmission grating*. Appl. Phys. Lett. 90 053501.
- L. Kuang, C. Wang, Z. W. (2010). *Quantum-dot-array diffraction grating with single order diffraction property for soft x-ray region*. Rev. Sci. Instrum. 81, 073508.
- M. Born, E. W. (1997). *Principles of Optics*. Cambridge U. Press, 7th ed.(expanded) edition.
- M. E. Warren, R. E. Smith, G. A. V. (1995). *High-efficiency subwavelength diffractive optical element in GaAs for 975 nm*. Opt. Lett. 20, 1441.
- V. Daneu, A. Sanchez, T. Y. F. (2000). *Narrowband operation of a pulsed dye laser without intracavity beam expansion*. J. Appl.Phys. 48, 4495.
- W. Goodman, J. (1996). *Introduction to Fourier Optics*. McGraw-Hill, 2nd edition.
- Y. Saitoh, H. Kimura, Y. S. (2000). *Performance of a very high resolution soft x-ray beamline BL25SU with a twin-helical undulator at SPring-8*. Rev. Sci.Instrum. 71, 3254.
- Y. W. Huang, S. T. Hu, S. Y. Y. (2004). *Tunable diffraction of magnetic fluid films and its potential application in coarse wavelength-division multiplexing*. Opt. Lett.29, 1867.